

## A model-independent constraint on the Hubble constant with gravitational waves from the Einstein Telescope

Sixuan Zhang

*Department of Astronomy, Beijing Normal University, Beijing 100875, China;*

Shuo Cao\*

*Department of Astronomy, Beijing Normal University, Beijing 100875, China;  
caoshuo@bnu.edu.cn*

Jia Zhang

*School of Physics and Electrical Engineering, Weinan Normal University, Shanxi 714099,  
China;*

Tonghua Liu

*Department of Astronomy, Beijing Normal University, Beijing 100875, China;*

Yuting Liu

*Department of Astronomy, Beijing Normal University, Beijing 100875, China;*

Shuaibo Geng

*Department of Astronomy, Beijing Normal University, Beijing 100875, China;*

Yujie Lian

*Department of Astronomy, Beijing Normal University, Beijing 100875, China;*

Received Day Month Year

Revised Day Month Year

In this paper, we investigate the expected constraints on the Hubble constant from the gravitational-wave standard sirens, in a cosmological-model-independent way. In the framework of the well-known Hubble law, the GW signal from each detected binary merger in the local universe ( $z < 0.10$ ) provides a measurement of luminosity distance  $D_L$  and thus the Hubble constant  $H_0$ . Focusing on the simulated data of gravitational waves from the third-generation gravitational wave detector (the Einstein Telescope, ET), combined with the redshifts determined from electromagnetic counter parts and host galaxies, one can expect the Hubble constant to be constrained at the precision of  $\sim 10^{-2}$  with 20 well-observed binary neutron star (BNS) mergers. Additional standard-siren measurements from other types of future gravitational-wave sources (NS-BH and BBH) will provide more precision constraints of this important cosmological parameter. Therefore, we obtain that future measurements of the luminosity distances of gravita-

2 *Zhang, et al.*

tional waves sources will be much more competitive than the current analysis, which makes it expectable more vigorous and convincing constraints on the Hubble constant in a cosmological-model-independent way.

*Keywords:* cosmological parameters - gravitational waves

PACS numbers:

## 1. Introduction

The Hubble constant  $H_0$ , which illustrates the expansion rate of the universe today, plays a significant role in the deep understanding of fundamental physics questions.<sup>1</sup> Therefore, precise and accurate measurement of the Hubble constant is one of the most fundamental issues influencing our understanding of the Universe. Although multiple paths to independent estimates of  $H_0$  have been accessed by many astrophysical probes - in particular the observations of type Ia supernovae (SNe Ia) and the first acoustic peak location in the pattern of anisotropies of the Cosmic Microwave Background Radiation (CMBR) - two issues should be reminded. First of all, the Hubble constant cannot be constrained directly from CMB observations, e.g. the latest Planck 2015 results,<sup>2</sup> but must be inferred by assuming a pre-assumed cosmological model (the standard  $\Lambda$ CDM model). It was found in<sup>3</sup> that many parameters (i.e., the matter density parameter  $\Omega_m$ ) become degenerate with the Hubble constant: a high value of  $\Omega_m$  will lead to a low value of  $H_0$ .

When relaxing the  $\Lambda$ CDM assumption by introducing an exotic source of matter with negative net pressure, the so-called dark energy to explain cosmic acceleration, the strong degeneracy between various cosmological parameters (such as the cosmic equation of state  $w = p/\rho$ , or the interaction term between dark matter and dark energy) and the Hubble constant was also noticed and discussed in.<sup>4-8</sup> Second, alternative methods of deriving the Hubble constant from cosmological-model-independent probes, focus on the luminosity distance  $D_L(z)$  using SNe Ia as standard candles at lower redshifts<sup>9</sup> and the time-delay distance  $D_{\Delta t}$  using time delays of strong lensing systems as standard rulers.<sup>10,11</sup> These results showed that recent determinations of  $H_0$ , from the Supernovae  $H_0$  for the Equation of State of Dark Energy (SH0ES) collaboration<sup>9</sup> and a joint analysis of six gravitationally lensed quasars with measured time delays,<sup>10</sup> are in strong tension with the Planck CMB measurements. The debate about the discrepancy between the Hubble constant measured locally and the value inferred from the Planck survey, has kept the discussion about a local underdensity alive.<sup>12</sup> Therefore, such tension may force the rejection of the standard  $\Lambda$ CDM model or indicate new physics incorporated into cosmology.

However, it is worth noting that all of these  $H_0$  measurements performed through electromagnetic (EM) radiations. Gravitational wave offers an independent method of determining  $H_0$  and resolving the  $H_0$  discrepancy.<sup>13</sup> The inspiraling and merging compact binaries consisting of neutron stars (NSs) and black holes (BHs), can be considered analogously as the supernovae (SNe) standard candles, namely the

standard sirens. The most well-established method for measuring  $H_0$  is through the Hubble law, based on the observations of the local Hubble flow velocity of a source and the distance to the source in the local Universe. Gravitational wave signals from inspiraling binary systems are “standard sirens” in that the absolute value of their luminosity distances, and thus the distances to GWs in the Hubble flow can be determined, and therefore can be used to infer  $H_0$  independent of any other distance ladders: standard sirens are self-calibrating. The local Hubble flow velocity is typically obtained via the identification of electromagnetic counterpart and the host galaxy. The breakthrough took place with the first direct detection of GW170817 in both gravitational waves and electromagnetic waves,<sup>14</sup> which has opened an era of gravitational-wave multi-messenger astronomy.<sup>15</sup> determined the Hubble constant to be  $H_0 = 70.0_{-8.0}^{+12.0}$  km/s/Mpc, which is well consistent with the currently existing measurements (CMB and SNe Ia). In the past years, many papers have studied the possibility of the GW as standard sirens,<sup>16–22</sup> and there are also estimations on the constraint ability of the Hubble constant by the simulated GW data.<sup>23–25</sup> Following this direction, extensive efforts have been made to use simulated GW data to place constraints on this important cosmological parameter,<sup>26</sup> which showed that the constraint ability of GWs is much better than the traditional probes (with a precision of approximately two percent), if hundreds of GW events have been observed by LIGO and Virgo within five years.

Inspired by the previous work,<sup>26</sup> in this paper we explore the ability of the gravitational wave detections of the Einstein Telescope(ET) to constrain the Hubble constant in a model-independent way based on the Hubble law. More importantly, the third-generation ground-based detector, i.e. Einstein telescope (ET), will be ten times more sensitive in amplitude than the advanced ground-based detectors, covering the frequency range of 1-10<sup>4</sup> Hz. Therefore, 10<sup>4</sup> – 10<sup>5</sup> GW events will be detected by ET per year and about one of a thousand events will locate in the low-redshift range of [0, 0.1].<sup>27</sup> This expected considerable number of low-redshift GW events implies that it is possible to use these systems for estimating the Hubble constant, by combining the measurements of the sources’ redshifts from, for example, the electromagnetic (EM) counterpart. In this paper, we explore the ability of the gravitational wave detections to constrain  $H_0$ . As result, we obtain that future results from GWs will be much more competitive with current limits from current analyses. The paper is organized as follows. In Section II we describe the methodology used in our work. The simulated GW data and the error estimation of the standard siren measurements are presented in Section III. In Section IV, we present the constraints these data put on the Hubble constant. Finally, the conclusions and discussions are presented in Section V. Throughout this paper, the Hubble constant  $H_0 = 70.0$ km/s/Mpc from the latest GW observations (GW170817) is taken for Monte Carlo simulations in our analysis.

4 *Zhang, et al.*

## 2. Methodology

We assume that in the homogeneous and isotropic universe, its geometry can be described by the Friedmann-Lemaître-Robertson-Walker (FLRW) metric

$$ds^2 = -dt^2 + \frac{a(t)^2}{1 - kr^2} dr^2 + a(t)^2 r^2 d\Omega^2, \quad (1)$$

where  $t$  is the cosmic time,  $a(t)$  is the scale factor whose evolution depends on the matter and energy contents of the universe, while  $k$  represents the spatial curvature.  $k = +1, -1, 0$  corresponds to closed, open, and flat universe, respectively and is related to the curvature parameter as  $\Omega_k = -k/H_0^2$ . In the framework of FLRW metric, at nearby distances the mean expansion rate of the Universe is well approximated by the expression<sup>28</sup>

$$v_H = H_0 D_H, \quad (2)$$

where  $v_H$  is the local Hubble flow velocity of a source,  $D_H$  is the Hubble distance to the source (all cosmological distance measures, such as luminosity distance, comoving distance and angular diameter distance can not be distinguished at low redshifts). In this case, the exact value of other cosmological parameters (such as the matter density parameter  $\Omega_m$ , the cosmic equation of state  $w$ ) is not our concern, since they are similarly insensitive to the distance measurements. In a closed universe, this linear redshift-distance relation is usually expressed in the form of  $cz = H_0 D_H$ , where  $c$  is the speed of light and  $z$  is the redshift of the galaxy.<sup>28</sup> However, with the exception of cosmological models in which the Hubble parameter is a constant at higher redshifts, the Hubble law is linear only for low redshifts ( $z \ll 1$ ).<sup>29</sup> When it comes to a higher redshift, such approximation can lead to a significant error in measuring  $D_H$  and one needs to consider the relativistic correction of the approximation,<sup>30</sup>  $1 + z = \sqrt{(1 + \frac{v}{c}/(1 - \frac{v}{c}))}$ . With this correction, the corrected Hubble law can be rewritten as<sup>31</sup>

$$\frac{(1+z)^2 - 1}{(1+z)^2 + 1} c = H_0 D_H. \quad (3)$$

More specifically, by taking the relativistic correction form, it is estimated that the observable distances (luminosity distance, angular diameter distance, etc.) will differ from the Hubble distance by less than 5% (when  $z \leq 2$ ).<sup>31</sup> In this paper, we choose to implement a stringent redshift criterion when the relativistic correction is considered (i.e.,  $z < 0.1$ ).

In order to calculate  $H_0$ , on the one hand, we must also measure a redshift for each binary merger. Throughout, we take the redshift  $z$  to be the peculiar-velocity-corrected redshift, i.e., the redshift of the source if it is located in the Hubble flow. It should be noted two different cases will be considered in this work: the GW sources are caused by binary merger of a neutron star with either a neutron star or black hole, which can generate an intense burst of  $\gamma$ -rays (SGRB) with measurable source redshift, or the redshift information either comes from a statistical analysis over a

catalogue of potential host galaxies, when the GW sources are caused by compact binaries consisting of black holes (BHs).

On the other hand, different from the luminosity distance measurements from EM observations, the GW signal from a compact binary system can provide the measurement in another way: through its dependency on the amplitude of the GW event and the so-called chirp mass of the binary system, which can be measured from the GW signals phasing.<sup>13</sup> More specifically, the GW signal from each detected binary merger (with component masses  $m_1$  and  $m_2$ ) provides a measurement of  $D_L$ , which can be directly inferred from the amplitude

$$\mathcal{A} = \frac{1}{D_L} \sqrt{F_+^2(1 + \cos^2(\iota))^2 + 4F_\times^2 \cos^2(\iota)} \times \sqrt{5\pi/96\pi^{-7/6} \mathcal{M}_c^{5/6}} \quad (4)$$

of Fourier transform of the strain  $h(t)$  of GW signal

$$\mathcal{H}(f) = \mathcal{A} f^{-7/6} \exp[i(2\pi f t_0 - \pi/4 + 2\psi(f/2) - \phi_{2.0})], \quad (5)$$

where  $t_0$  is the epoch of the merger, while the definitions of the functions  $\psi$  and  $\varphi_{(2.0)}$  can be found in.<sup>19</sup> In the transverse-traceless (TT) gauge, the strain can be written as the linear combination of the two polarization states

$$h(t) = F_\times(\theta, \phi, \psi) h_\times(t) + F_+(\theta, \phi, \psi) h_+(t) \quad (6)$$

where  $h_\times$  and  $h_+$  are the two independent components of the GW tensor,  $F_\times$  and  $F_+$  are the beam pattern functions,  $\psi$  denotes the polarization angle, and  $(\theta, \phi)$  are the location angles of the source in the sky, which describes the location of the source relative to the detector. The exact forms of pattern functions for ET are given by<sup>19</sup>

$$\begin{aligned} F_+^{(1)}(\theta, \phi, \psi) &= \frac{\sqrt{3}}{2} \left[ \frac{1}{2} (1 + \cos^2(\theta)) \cos(2\phi) \cos(2\psi) \right. \\ &\quad \left. - \cos(\theta) \sin(2\phi) \sin(2\psi) \right], \\ F_\times^{(1)}(\theta, \phi, \psi) &= \frac{\sqrt{3}}{2} \left[ \frac{1}{2} (1 + \cos^2(\theta)) \cos(2\phi) \sin(2\psi) \right. \\ &\quad \left. + \cos(\theta) \sin(2\phi) \cos(2\psi) \right]. \end{aligned} \quad (7)$$

and the other two interferometer's antenna pattern functions are  $F_{+,\times}^{(2)}(\theta, \phi, \psi) = F_{+,\times}^{(1)}(\theta, \phi + 2\pi/3, \psi)$  and  $F_{+,\times}^{(3)}(\theta, \phi, \psi) = F_{+,\times}^{(1)}(\theta, \phi + 4\pi/3, \psi)$ , since the three interferometers of the ET are arranged in an equilateral triangle. We can define the chirp mass  $\mathcal{M}_c = M\eta^{3/5}$  and its corresponding observational counterpart as  $\mathcal{M}_{c,\text{obs}} = (1+z)\mathcal{M}_{c,\text{phys}}$  (with the total mass  $M = m_1 + m_2$  and the symmetric mass ratio  $\eta = m_1 m_2 / M^2$ ).  $\iota$  is the angle between inclination of the binary system's orbital angular momentum and line of sight. One should note that, from observational point of view, the maximal inclination is about  $\iota = 20^\circ$  and averaging the

6 *Zhang, et al.*

Fisher matrix over the inclination  $\iota$  with the limit  $\iota < 20^\circ$  is approximately equivalent to taking  $\iota = 0$ . Therefore, one can take  $\iota = 0$  for simplicity, as argued in<sup>32</sup> and references therein.

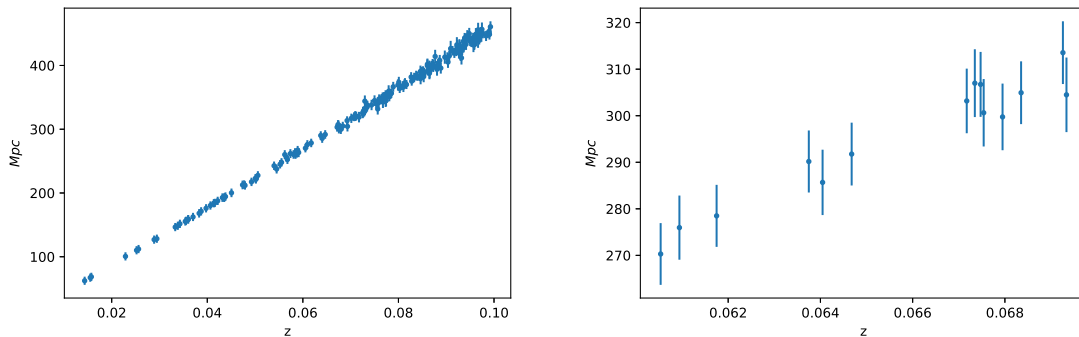


Fig. 1. The luminosity distance measurements from 200 low-redshift GW events generated from inspiraling binary neutron stars (left panel). Details of the measurements in the redshift range 0.06–0.07 are also shown for comparison (right panel).

### 3. Simulation and error estimation

In this section we simulate GW events based on the Einstein Telescope, the third generation of the ground-based GW detector. In the simulation, the mass distribution of NS is chosen to be uniform in the interval of  $[1.4, 2.4] M_\odot$ . We adopt the redshift distribution of the GW sources observed on Earth, which can be written as<sup>19</sup>

$$P(z) \propto \frac{4\pi D_c^2(z) R(z)}{H(z)(1+z)}, \quad (8)$$

where  $H(z)$  is the Hubble parameter of the fiducial cosmological model,  $D_c(z)$  is the co-moving distance at redshift  $z$ , and  $R(z)$  represents the time evolution of the burst rate taken as<sup>33</sup>

$$R(z) = \begin{cases} 1 + 2z, & z \leq 1 \\ \frac{3}{4}(5 - z), & 1 < z < 5 \\ 0, & z \geq 5. \end{cases} \quad (9)$$

For the network of three independent ET interferometers, the combined signal-to-noise ratio (SNR) of the GW waveform is

$$\rho = \sqrt{\sum_{i=1}^3 \langle \mathcal{H}^{(i)}, \mathcal{H}^{(i)} \rangle}. \quad (10)$$

Here the inner product is defined as

$$\langle a, b \rangle = 4 \int_{f_{\text{lower}}}^{f_{\text{upper}}} \frac{\tilde{a}(f)\tilde{b}^*(f) + \tilde{a}^*(f)\tilde{b}(f)}{2} \frac{df}{S_h(f)}, \quad (11)$$

where  $\tilde{a}(f)$  and  $\tilde{b}(f)$  are the Fourier transforms of the functions  $a(t)$  and  $b(t)$ .  $S_h(f)$  is the one-side noise power spectral density (PSD) characterizing the performance of a GW detector

$$S_h(f) = S_0[x^{p1} + a_1x^{p2} + a_2f(x)] \quad (12)$$

where  $f(x)$  takes the form as

$$f(x) = \frac{1 + b_1x + b_2x^2 + b_3x^3 + b_4x^4 + b_5x^5 + b_6x^6}{1 + c_1x + c_2x^2 + c_3x^3 + c_4x^4} \quad (13)$$

with the definition of  $x = f/200$ .<sup>19</sup> The lower cutoff frequency  $f_{\text{lower}}$  is fixed at 1 Hz. The upper cutoff frequency,  $f_{\text{upper}}$ , is decided by the last stable orbit (LSO),  $f_{\text{upper}} = 2f_{\text{LSO}}$ , where  $f_{\text{LSO}} = 1/(6^{3/2}2\pi M_{\text{obs}})$  is the orbit frequency at the LSO, and  $M_{\text{obs}} = (1 + z)\mathcal{M}_{\text{phys}}$  is the observed total mass. Meanwhile, the signal is identified as a GW event only if the ET interferometers have a network SNR of  $\rho > 8.0$ .<sup>25</sup>

Different sources of uncertainties are included in our simulation of luminosity distance  $D_L$ . Firstly, in the standard framework of GW data analysis, the information of relevant parameters ( $\theta$ ) are derived by fitting the frequent-domain wave model  $h(f; \theta)$  to the frequent-domain detector data  $d(f)$ . If the noise is stationary and Gaussian, the likelihood function  $\mathcal{L}$  is defined as<sup>34</sup>

$$\ln \mathcal{L} = -\frac{1}{2} \int_0^\infty df \frac{|d(f) - h(f; \theta)|^2}{S_h(f)} \quad (14)$$

where  $d(f)$  and  $S_h(f)$  are implicit functions of the calibration parameters ( $\lambda$ ). Specially, considering the difference between the detector's true calibration parameters ( $\lambda_{\mathbf{t}}$ ) and the calibration parameters used to produce the strain data from power fluctuations ( $\lambda$ ), the generated calibration error should be included into the parameter estimation pipeline, described by the parameter  $\Delta\lambda = \lambda - \lambda_{\mathbf{t}}$ . In this analysis, we take the calibration-induced error ( $\sigma_{D_L}^{\text{cal}}$ ) as one third of the noise-induced error ( $\sigma_{D_L}^{\text{noi}}$ ), when the parameter estimation is dominated by systematics induced by detector noise.<sup>35</sup>

Secondly, when the error on luminosity distance is uncorrelated with errors on the remaining GW parameters, the noise-induced error can be estimated with Fisher matrix by<sup>36</sup>

$$\sigma_{D_L}^{\text{noi}} \simeq \sqrt{\left\langle \frac{\partial \mathcal{H}}{\partial D_L}, \frac{\partial \mathcal{H}}{\partial D_L} \right\rangle^{-1}}, \quad (15)$$

It should be pointed out that in the ET era, we will be confronted with a family of phenomenological waveforms that incorporates the dynamics of the inspiral, merger, and ringdown phases of the coalescence,<sup>37,38</sup> while the inclusion of the merger phase

8 *Zhang, et al.*

and ringdown phase may helpfully break the degeneracy between the luminosity distance  $D_L$  and inclination angle  $\iota$ .<sup>39,40</sup> In this paper, following the procedure extensively applied in the literature,<sup>20,25</sup> we focus only on the inspiral phase of the GW signal, with the corresponding instrumental error written as

$$\sigma_{D_L}^{\text{inst}} = \sqrt{(\sigma_{D_L}^{\text{noi}})^2 + (\sigma_{D_L}^{\text{cal}})^2} \quad (16)$$

where  $\sigma_{D_L}^{\text{noi}}$  is the noise-induced error that can be estimated as  $\sigma_{D_L}^{\text{noi}} \simeq \frac{2D_L}{\rho}$ .<sup>34,36</sup> Note that the maximal effect of the inclination on the SNR is a factor of 2 (between  $\iota = 0^\circ$  and  $\iota = 90^\circ$ ), for a conservative estimation of the correction between  $D_L$  and  $\iota$ .

Thirdly, following the strategy described by,<sup>25</sup> weak lensing has been estimated as a major source of error on  $D_L(z)$  for standard sirens. For the ET we estimate the uncertainty from weak lensing according to the fitting formula of  $\sigma_{D_L}^{\text{lens}}/D_L = 0.05z$ .<sup>19</sup> Therefore, the distance precision per GW is taken to be

$$\sigma_{D_L}^{\text{sta}} = \sqrt{(\sigma_{D_L}^{\text{inst}})^2 + (\sigma_{D_L}^{\text{lens}})^2}. \quad (17)$$

Finally, precise redshift measurements are the crucial point of our idea. We consider two cases: In the with-counterpart case, with the observation of the EM counterpart, the redshift of a GW event can be determined. We assume that the EM counterpart is close enough to its host galaxy that the host can be unambiguously identified, and we can measure its sky position and redshift. In the previous works,<sup>20–22,25</sup> the uncertainty of the redshift measurement is always ignored, because it is ignorable compared to the uncertainty of the luminosity distance. However, in the case of local universe, the redshift uncertainty caused by the uncertainty of peculiar velocity should be taken into account. Throughout this paper, we take the redshift  $z$  to be the peculiar-velocity-corrected redshift (i.e., the redshift of the source located in the Hubble flow) and apply two different cases. Following the procedure performed in the recent analysis,<sup>26</sup> a standard deviation of  $c\sigma_z = 200$  km/s is assumed for each BNS and BH-NS system (with a direct EM counterpart), which is a typical uncertainty for the peculiar velocity correction well consistent with the peculiar velocity measurement of NGC 4993 (the host galaxy of GW170817).<sup>41</sup> Note that the recent analysis of BH-NS mergers has discussed the possibility that the neutron star can be tidally disrupted and emit electromagnetic radiation, depending on the mass ratio and the black hole spin.<sup>42</sup> For the latter case in which the host galaxy of a GW event can not be identified (BBH), the redshift comes from a statistical analysis over a catalogue of potential host galaxies, which will be discussed later.

Now the final key question required to be answered is: how many low-redshift GW events can be detected per year for the ET? Focusing on the GW sources caused by binary merger of neutron stars (with detectable EM counterpart measurable source redshift), it is revealed that the third generation ground-based GW detector can detect up to  $10^3 - 10^7$  events, with the upper detection limit of  $z \sim 2.0$ .<sup>27</sup>

Following our detailed calculation that only 0.1% of the total GW events will be located in the redshift range of  $[0, 0.1]$ , one may expect that  $1 - 10^4$  low-redshift events could be used in our analysis. In addition, recent analysis revealed that the five-detector network including LIGO, Virgo, KAGRA and LIGO-India plans to detect  $\sim 40$  events per year, if the designed sensitivity of the network could be achieved in the future.<sup>26</sup> Therefore, assuming the luminosity distance measurements obey the Gaussian distribution, we simulate 200 GW events of BNS merging used for statistical analysis in the next section, the redshift distribution of which is shown in Fig. 1.

We summarize the main route of our method as follows:

- Simulate 200 GW events according to the redshift distribution in Eq. (8). The angles describing the position of each BNS system are randomly sampled within the interval of  $\theta \in [0, \pi)$  and  $\phi \in [0, 2\pi)$ .
- Calculate the luminosity distance  $D_L(z)$  according to Eq. (2)-(3). Randomly sample the mass of neutron star within  $[1.4, 2.4]M_\odot$ . Evaluate the signal-to-noise ratio (SNR) and the error  $\sigma_{D_L}$  when the SNR of the detector network reaches above 8.
- For a confirmed GW event, the statistical error of luminosity distance  $\sigma_{D_L}^{\text{sta}}$  can be figured out through Eq. (17). Moreover, considering the effect of the peculiar velocity of the host galaxy  $v_{\text{pec}}$ , we also add the systematical uncertainty of observed redshift  $z_{\text{obs}}$  to project uncertainties  $\sigma_{D_L}^{\text{sys}}$  onto the final uncertainty of distance estimation (Eq. (3)). We therefore take the total uncertainty on the luminosity distance as  $\sigma_{D_L}^{\text{tot}} = \sqrt{(\sigma_{D_L}^{\text{sta}})^2 + (\sigma_{D_L}^{\text{sys}})^2}$ . The observed luminosity distance  $D_L$  follows a Gaussian distribution whose mean is  $D_L^{\text{fid}}$  and variance is  $\sigma_{D_L}^{\text{tot}}$ , i.e.,  $D_L \sim \mathcal{N}(D_L^{\text{fid}}, \sigma_{D_L}^{\text{tot}})$ .

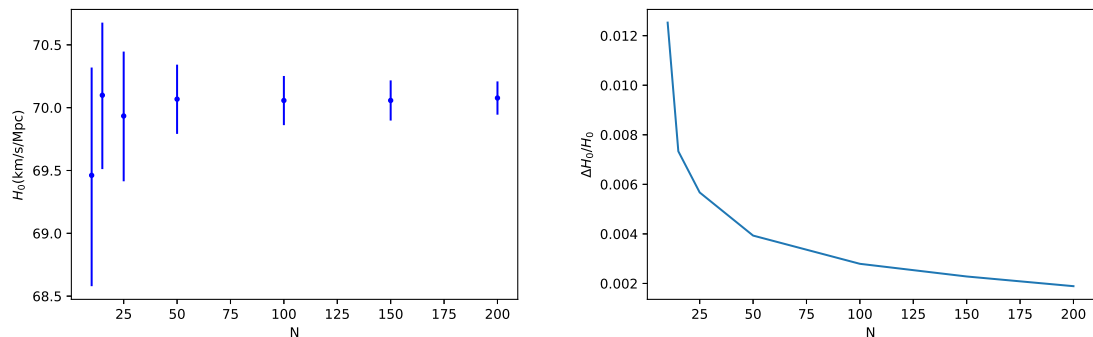


Fig. 2. Left: Inferred Hubble constant as a function of the number of GW events (BNS mergers with EM counterparts). Right: The corresponding precision of the Hubble constant constraints for a variable number of GW events (BNS mergers with EM counterparts).

#### 4. Results and discussions

In order to place constraints on the Hubble constant with MCMC method, the likelihood estimator is determined by  $\chi^2$  statistics

$$\chi^2 = \sum_{i=1}^N \left( \frac{D_L^{obs}(z_i) - D_L^{th}(z_i)}{\sigma_{D_L,i}} \right)^2 \quad (18)$$

where  $N$  denotes the number of data sets,  $D_L^{th}$  is the predicted luminosity distance value in the Hubble law and  $D_L^{obs}$  is the measured value with a uncertainty of  $\sigma_{D_L}$  in the simulated data.

Fig. 2 shows the precision of the curvature parameter assessment as a function of GW sample size for future ET detector, where weighted means and corresponding standard deviations are illustrated for comparison. Projected fractional error for the standard siren  $H_0$  measurement for BNSs is also shown. One can see that, even with about 20 well-observed GW events due to BNS mergers one can expect the Hubble constant to be estimated with the precision of  $\delta H_0 \sim 1\%$  (at the  $1\sigma$  level), if it is possible to independently measure a unique redshift for all BNS events. More importantly, we find that in this counterpart case, the fractional  $H_0$  uncertainty will be proportional to  $1/\sqrt{N}$ , where  $N$  is the number of BNS mergers detected by the ET. Still, there are several remarks that remain to be clarified as follows.

Firstly, in the above analysis we assume that EM counterparts are detectable for all BNS systems. For example, as GW170817 demonstrated, for the merger of a BNS system it is possible to identify a kilonova counterpart independently of the short  $\gamma$  ray burst (SGRB). These EM counter parts can help us in locating the events in the sky and identifying the host galaxy of the event,<sup>43</sup> and the locating ability can be improved with the use of H.E.S.S.Imaging Air Cherenkov Telescopes(IACTs).<sup>44</sup> However, from observational point of view we don't expect to observe EM counter parts for all GW events. For example, the optical counter parts, kilo-nova, are too dim to be observed in large luminosity distance. More specifically, SGRBs are strongly beamed phenomena which carry a great deal of energy and we can only detect them when they are almost face-on, which will significantly decline the number of detectable GW events with SGRB.<sup>45</sup> Following the recent discussion of GW170817, the eject matter from a merging BNS system can cause a secondary radiation which might power the radiation for a longer time and a wider radiation angle. This suggest that only 10% of the 200 BNS events detected by ET will be available with the EM counterparts such as SGRB.<sup>26</sup> Therefore, after about 20 gravitational-wave standard sirens, the fractional uncertainty on  $H_0$  could still reach 1% (at the  $1\sigma$  level) by the end of five years of ET at design sensitivity, sufficient to arbitrate the current tension between local and high- $z$  measurements of  $H_0$ .

Secondly, besides BNS with EM counterparts, there are other types of GW sources that can contribute in providing precise determination of the Hubble constant. Theoretically, ET could also detect a large number of GW signals for black

hole - neutron star (BH-NS) merger systems and binary black hole (BBH) merger systems. These two types of GW sources are also of concern to our investigation in this paper. While we do not expect EM counterpart from BBH systems, we do want to observe the EM counterpart from BN-BH systems, and the optical luminosity depends on the property of the neutron star.<sup>46</sup> For the former type, the electromagnetic (EM) signals are emitted during the merger processes, allowing us to determine the redshift of sources. In the framework of ET project, the expected detect rate of BNS and BHNS are in the same order of  $10^3$  to  $10^7$ .<sup>27</sup> Therefore, it is reasonable to assume that with the observation of 20 BNS merger with EM counterparts, one can detect 20 BHNS merger with their EM counterparts as well. For the latter case where a unique counterpart cannot be identified for a BBH merger, it is possible to carry out a measurement of the Hubble constant using the statistical approach, i.e., there are still other methods to identify their host galaxies, in a statistical way which might not be that accurate.<sup>27</sup> More specifically, we will apply the methodology proposed in,<sup>26</sup> in which a galaxy catalogue is used to describe all potential host galaxies in the case that the EM counterpart is absent. The simulated galaxy catalogue is constructed by distributing galaxies uniformly in the co-moving volume of  $10000 \text{ Mpc}^3$  with a number density of  $0.02 \text{ Mpc}^{-3}$ , each of which has the same probability to be the host galaxy of the GW event. Given the detailed calculation presented in,<sup>26</sup> after two years of full operation, the LIGO and Virgo network is expected to detect  $\sim 16$  BBH events (with well estimation of statistical redshifts) in the local universe (located in the volume of  $10000 \text{ Mpc}^3$ ), which will lead to a 10% of Hubble constant measurement. Therefore, it is reasonable to simulate 30 BBH systems with redshift determination in the framework of ET configurations (in the simulation, the mass distribution of BH is chosen to be uniform in the interval of  $[3, 10] M_{\odot}$ <sup>21, 22</sup>). A representative result is illustrated in Fig. 3, in order to compare the  $H_0$  constraints with different types of gravitational-wave events. The left panel is obtained using BNS GW sirens, while the middle panel is obtained using BHNS sirens, which is compared in the right panel with BBH GW sirens, respectively. As was noted in the previous work based on the LIGO and Virgo network,<sup>26</sup> the error bars will be greatly reduced when different types of GW events are included. Meanwhile, benefit from a larger total mass and smaller merger frequency than BNS, one could also expect a larger SNR for a specific BHNS event, which will greatly contribute to the distance measurements and thus the standard siren  $H_0$  constraint.<sup>42</sup> However, constraints from BBH systems without counterparts are inferior, due to the larger number of potential host galaxies compared with other two types of GW events.<sup>26</sup>

Now it is worthwhile to compare our forecast results with some previous  $H_0$  tests fitting the Hubble constant in different cosmological models, based on the “ $D_L - z$ ” relation at higher redshifts in the GW domain. Using the information of luminosity distances and redshifted chirp masses for a catalog of BNSs detected by an advanced era network,<sup>24</sup> studied a technique to obtain constraints on the

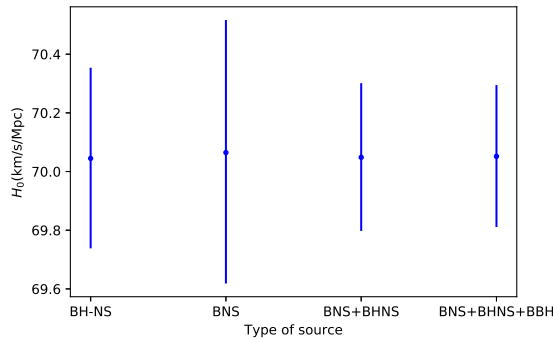


Fig. 3. Constraints on the Hubble constant with three types of GW sources, 20 BNS with EM counterparts, 20 BH-NS with EM counterparts, and 30 BBH without EM counterparts but with well-estimated statistical redshifts.

Hubble constant and NS mass-distribution parameters simultaneously. It was found that  $H_0$  could be estimated at the precision of 10% with  $\sim 100$  such kind of GW events. Meanwhile, in the framework of a range of ground-based detector networks,<sup>23</sup> examined how well distances (and thus cosmological parameters) can be measured from BNSs with electromagnetic counterparts (such as the associated SGRB). The analysis results revealed that  $H_0$  could be measured with a fractional error of  $\sim 13\%$  with 4 GW-SGRB events, which could be improved to  $\sim 5\%$  with 15 events detected by the advanced LIGO-Virgo detector network. Focusing on constraint ability of the third-generation gravitational wave detector (the Einstein Telescope), the recent analysis showed that with the simulated data of 500 standard sirens, one can constrain the Hubble constant with an accuracy comparable to the most recent Planck results.<sup>25</sup> By considering our results and those from,<sup>23–25</sup> our results show that strong constraints on the Hubble constant can be obtained in a cosmological-model-independent fashion. Such conclusion agrees very well with that obtained in the framework of LIGO-Virgo detector network.<sup>26</sup>

Measuring the Hubble constant ( $H_0$ ) independent of CMB observations is one of the most important complementary probes for understanding the nature of the Universe. Therefore, the fractional uncertainty on  $H_0$  will reach 1% by the end of five years of ET at design sensitivity, which furthermore strengthens the probative power of the third generation ground-based GW detectors to inspire new observing programs or theoretical work in the moderate future. Finally, one should note that, in order to achieve this goal, dedicated observations of the sky position of each host galaxy (that is, with negligible measurement error) would be necessary. Although the GW distance posterior changes slowly over the sky and therefore is not sensitive to the precise location of the counterpart, obtaining such measurements for a sample of different types of GW events would require substantial follow-up efforts, which can lead to significant improvements in the distance, and hence  $H_0$  measure-

ments. We also hope future observational data such as strongly lensed gravitational waves (GWs) from compact binary coalescence and their electromagnetic (EM) counterparts systems,<sup>47,48</sup> precise measurements of the Hubble parameter obtained by cosmic chronometer and radial BAO size methods,<sup>49–51</sup> and VLBI observations of compact radio quasars with higher sensitivity and angular resolution<sup>52–55</sup> may improve remarkably the constraints on this key cosmological parameter.

### Acknowledgments

We are grateful to Jingzhao Qi for helpful discussions. This work was supported by National Key R&D Program of China No. 2017YFA0402600, the National Natural Science Foundation of China under Grants Nos. 11690023, 11373014, and 11633001, the Strategic Priority Research Program of the Chinese Academy of Sciences, Grant No. XDB23000000, the Interdiscipline Research Funds of Beijing Normal University, and the Opening Project of Key Laboratory of Computational Astrophysics, National Astronomical Observatories, Chinese Academy of Sciences.

### References

1. Weinberg, D. H., et al. *Phys. Rep.*, 530, 87 (2013)
2. Ade, P. A. R., et al. (Planck Collaboration), *A&A*, 594, A13 (2016)
3. Cao, S., et al. *A&A*, 606, A15 (2017)
4. Cao, S., Liang N., & Zhu, Z.-H. *MNRAS*, 416, 1099 (2011)
5. Cao, S. & Liang, N. *IJMPD*, 22, 1350082 (2013)
6. Cao, S., et al. *IJTP*, 54, 1492 (2015)
7. Chen, Y., et al. *JCAP*, 02, 010 (2015)
8. Pan, Y., et al. *ApJ*, 808, 78 (2015)
9. Freedman, W. L. *Nature Astronomy*, 1, 0121 (2017)
10. Wong, K. C., et al. *arXiv:1907.04869*
11. Pan, Y., et al. *IJMPD*, 25, 1650003 (2016)
12. Riess, A. G., et al. *ApJ*, 876, 85 (2019)
13. Schutz, B. F. *Nature*, 323, 310 (1986)
14. Abbott, B. P., et al. (LIGO Scientific and Virgo Collaborations), *PPL*, 116, 061102 (2016)
15. Abbott, B., et al. (LIGO Scientific and Virgo Collaborations), 2017, *Nature*, 551, 85
16. Holz, D. E. & Hughes, S. A., *ApJ*, 629, 15 (2005)
17. MacLeod, C. L. & Hogan, C. J., *Phys. Rev.*, 77, 043512 (2008)
18. Sathyaprakash, B. S., et al. *CQG*, 27, 215006 (2010)
19. Zhao, W., et al. *PRD*, 83, 023005 (2011)
20. Cai, R.-G., et al. *arXiv:1509.06283*
21. Qi, J. Z., et al. *PRD*, 99, 063507 (2019)
22. Qi, J. Z., et al. 2019, *PDU*, 26, 100338 (2019)
23. Nissanke, S., et al. *ApJ*, 725, 496 (2010)
24. Taylor, S. R., Gair, J. R., & Mandel, I. *PRD*, 85, 023535 (2012)
25. Cai, R.-G. & Yang, T. *PRD*, 95, 044024 (2017)
26. Chen, H.-Y., et al. *Nature*, 562, 545 (2018)
27. The Einstein Telescope Project, <https://www.et-gw.eu/et/>
28. Hubble, E. *PNAS*, 15, 168 (1929)

14 *Zhang, et al.*

29. Harrison, E. *ApJ*, 403, 28 (1993)
30. Hogg, D. W. *arXiv:9905116v4*
31. Carroll, B. W. & Ostlie, D. A., *An Introduction to Modern Astrophysics* (2nd Edition), p1056, Cambridge University Press (2007)
32. Cai, R.-G., et al. *PRD*, 97, 103005 (2018)
33. Schneider, R., et al. *MNRAS*, 324, 797 (2001)
34. von Toussaint, U. *Rev. Mod. Phys.* 83, 943 (2011)
35. Hall, E. D., et al. *arXiv:1712.09719*
36. Cutler, C. & Holz, D. E. *PRD*, 80, 104009 (2009)
37. Husa, S., et al. *PRD*, 93, 044006 (2016)
38. Khan, S., et al. *PRD*, 93, 044007 (2016)
39. McWilliams, S. T., Lang, R. N., Baker, J. G., & Thorpe, J. I. *PRD*, 84, 064003 (2012)
40. Klein, A., et al. *PRD*, 93, 024003 (2016)
41. Nicolaou, C., Lahav, O., Lemos, P., Hartley, W., and Braden, J. *arXiv:1909.09609*
42. Vitale, S. & Chen, H. Y. *PRL*, 112, 251101 (2018)
43. Nakar, E. *Phys. Rep.* 442, 166 (2007)
44. Monica Seglar-Arroyo, M., et al. [The H.E.S.S Collaboration], *arXiv:1908.08822v1*
45. Rezzolla, L., et al. *ApJL*, 732, L6 (2011)
46. Barbieri, C., et al. *arXiv:1908.08822v1*
47. Liao, K., et al. *Nature Communications*, 8, 1148 (2017)
48. Cao, S., et al. *NatSR*, 9, 11608 (2019)
49. Ding, X., et al. *ApJL*, 803, L22 (2015)
50. Zheng, X., et al. *ApJ*, 825, 17 (2016)
51. J.-Z. Qi, et al. *RAA*, 18, 66 (2018)
52. Cao, S., et al. *EPJC*, 78, 749 (2018)
53. Cao, S., et al. *PDU*, 24, 100274 (2019)
54. Xu, T. P., et al. *JCAP*, 06, 042 (2018)
55. Ma, Y. B., et al. *EPJC*, 79, 121 (2019)